Theor Chim Acta (1992) 82: 299–308

Theoretica Chimica Acta

Electronic structure and the unimolecular reactions of imine peroixde HNOO*

Takayuki Fueno, Keiichi Yokoyama, and Shin-ya Takane
Department of Chemistry, Faculty of Engineering Science, Osaka University, Toyonaka, Osaka 560, Japan

Received May 1, 1991/Accepted October 2, 1991

Summary. Electronic structure and possible unimolecular reaction paths of a linear four-atom molecule HNOO to be formed by the addition of $NH(^3\Sigma^-)$ toward $O_2(^3\Sigma_g^-)$ are investigated by the SCF and MRD-CI calculations employing the 6-31G** basis functions. HNOO in its ground state ($^1A'$) is an ozone-like diradicaloid, whose N–O binding energy is only 27 kJ/mol. Geometries and excitation energies of various diradical (excited) states, both singlet and triplet, are examined. The isomerization paths of the ground-state HNOO($^1A'$) are traced by a multi-configuration (MC) SCF procedure and the activation barrier heights evaluated by the CI treatment. It has proved that energetically the most favorable is the 1,3-hydrogen migration to give hydroperoxynitrene NOOH($^1A'$) with the barrier height of 62 kJ/mol. The nitrene should be extremely unstable; it is liable to be decomposed to NO + OH with virtually no activation barrier.

Key words: Imine peroxide (HNOO) – Diradicaloid – Diradicals – 1,3-Hydrogen migration – Hydroperoxynitrene (NOOH)

1 Introduction

In these past years, we have concerned ourselves with the investigations of the reactions of the imino radical NH theoretically [1] as well as experimentally. The reaction of NH with O_2 in the gas phase is of interest along this line and seems to be of importance as well in relation to the chemistry of fuel combustions. The reaction has already received interest of experimental kineticists. Thus, Zetzsch and Hansen were the first group of workers who measured the rate of the reaction between $NH(^3\Sigma^-)$ and $O_2(^3\Sigma_g^-)$ [2]. The reaction has long been known to give NO and OH simultaneously during the decay of $NH(^3\Sigma^-)$ [3]. Recently, Hack et al. traced the same reaction by monitoring the laser-induced fluorescence of OH as well as $NH(^3\Sigma^-)$, to conclude that the activation energy is 6.4 kJ/mol in the temperature range 286–543 K [4].

* Presented at the 7th International Congress on Quantum Chemistry, Menton, July 1991

Naively, the reaction is expected to involve an initial association:

$$NH + O_2 \rightarrow HNOO \quad (1)$$

Little is known, however, as to the structural characteristics of HNOO, except for the possibility that there can exist various conformations for its diradical form [5]. Still less has been noted regarding the dynamical path of its isomerization/fragmentation process:

$$HNOO \rightarrow NO + OH \quad (2)$$

In the present work, we examine Eqs. (1) and (2) by *ab initio* computations. We will first optimize geometries of the various diradical (excited) states of HNOO as well as the singlet ground state, and estimate the electronic excitation energies. The paths of isomerization reactions of the ground-state HNOO will then be traced by the multi-configuration (MC) SCF procedure. The activation barrier heights are calculated by the multi-reference double-excitation (MRD) configuration-interaction (CI) method. In the light of the results of theoretical calculations, possible pathways for Eq. (2) will be discussed.

2 Method of calculation

Geometry optimizations of HNOO diradicals were carried out by the UHF SCF procedure using the Gaussian 82 program package [6]. For the ground state of HNOO($^1A'$) in particular, multi-configuration (MC) SCF method has been adopted, since its electron structure is basically of the closed-shell type and yet involves contributions of doubly-excited configurations to an unignorable extent. In practice, we used for the sake of convenience the limited-configuration formalism in which six electrons are accommodated in six frontier orbitals with the remaining electrons frozen in the low-lying molecular orbitals. Paths of the isomerization of HNOO($^1A'$) were traced by the same MC SCF procedure. The basis sets employed are throughout the conventional 6-31G functions [7] augmented with one set each of *d* or *p* polarization functions for every atom involved.

MRD-CI calculations were performed for all the stationary geometries located. The TABLE MRD-CI program furnished by Buenker [8, 9] was used. The configuration-selection and extrapolation routines were followed [10]. The maximal dimension of the configuration space used was ca. 10,000. The extrapolated CI energies were all subjected to the Langhoff–Davidson corrections [11], to estimate the full CI limit values. Since the corrected CI energies are relatively insensitive to the number of the reference configurations chosen, we adopt them as the ultimate CI energies and will denote them as E_{CI}. Other technical details of the MRD-CI calculations carried out here are the same as those described in our previous work on S_2O [12] and CH_2CH_2NH [1e].

3 Results

3.1 Ground singlet state

The HNOO molecule in its ground electronic state is a planar four-π-electron

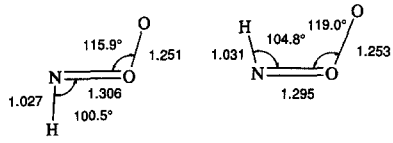

Fig. 1. Geometries of *trans*- and *cis*-HNOO($\tilde{X}^1A'$) optimized by the 6-electron-6-orbital MC SCF procedure employing the 6-31G** basis functions. The bond lengths are given in units of Å

system (A'). Preliminary MRD-CI calculations have revealed that it involves the contribution (squared weight $|c_i|^2$) of the ground configuration

$$\tilde{X}^1A';\quad (1a')^2\ldots(10a')^2(1a'')^2(2a'')^2$$

amounting only to 0.82. The contribution of the configuration arising from the two-electron transition $(2a'')^2\rightarrow(3a'')^2$ is as large as 0.06. The state is thus regarded as a diradicaloid as in the case of O_3 and hence cannot be described properly by the conventional RHF formalism.

Under such circumstances, the ground $^1A'$ state was subjected to the limited-space (6-electron/6-orbital) MC SCF calculations to optimize its geometry. The structures, *trans* and *cis*, thus optimized are shown in Fig. 1.

Results of MRD-CI calculations at these optimized geometries are given in Table 1. Both of them may be regarded as zwitter-ionic O-oxides of hydrogen nitrosyl HNO, which however possess a certain extent of diradical character. Relative stabilities of the geometric isomers are somewhat hard to assess: in both the RHF and MC SCF calculations, *trans*-HNOO is predicted to be 18 kJ/mol *less* stable than its *cis* isomer, whereas in the CI treatments the *trans* isomer is calculated to be *more* stable by 3 kJ/mol. Incidentally, the binding energy for the *cis* isomer against its decomposition into $NH(^3\Sigma^-) + O_2(^3\Sigma_g^-)$ is calculated to be 48 kJ/mol at the CI level. Upon correction for the vibrational zero-point energy, it reduces to 27 kJ/mol.

Table 1. Results of the MRD-CI calculations for *trans*- and *cis*-HNOO($\tilde{X}^1A'$)[a]

	trans	*cis*
Energies, $E + 204$ (hartree)		
RHF SCF	−0.47248	−0.47961
MC SCF[b]	−0.58496	−0.58559
CI, $T\rightarrow 0$[c]	−0.99895	−0.99767
CI, "full"	−1.04677	−1.04563
Configurations, $\|c_i\|^2$		
Closed[d]	0.8214	0.8309
$(2a'')^2\rightarrow(3a'')^2$	0.0581	0.0480
$(1a'')^2\rightarrow(3a'')^2$	0.0032	0.0034
$(2a'')\rightarrow(3a'')$	0.0059	0.0078
$(1a'')\rightarrow(3a'')$	0.0033	0.0028
$(7a')(1a'')\rightarrow(13a')(3a'')$	0.0033	0.0022

[a] Geometries are given in Fig. 1

[b] Based on the limited-space (6-electron/6-orbital) approximation

[c] The minimal threshold value adopted for the configuration selection is $T_{\min} = 20\ \mu$hartree, which corresponds to 9928 configurations chosen out of a total of 294525 symmetry-adapted configurational functions

[d] See text

3.2 Diradical (*excited*) states

The low-lying excited states are all diradical in character. The most fundamental of these is a diradical such that the two odd electrons are localized on the $p\pi$ orbitals of the nitrogen and the oxygen atoms, which may be termed the $\pi\pi$ state [5]. Above the $\pi\pi$ state, there can exist those diradical states in which either one of the $p\pi$ orbitals of the N and O atoms is occupied by an electron, leaving the other electron in an in-plane n orbital of N or O. Such states having one π-electron localized on either of the N and O atoms will be referred to as the $\pi\sigma$ and $\sigma\pi$ states, respectively [5]. Further, the state in which both $p\pi$ orbitals are occupied by a pair of electrons so that both the in-plane n orbitals constitute the radical sites is also conceivable. This last state may be referred to as the $\sigma\sigma$ state [5]. Taking the ground configuration as the standard, the principal configurations of these various states are represented as follows:

$$\pi\pi(A'); \quad (2a'') \rightarrow (3a'')$$
$$\pi\sigma(A''); \quad (10a') \rightarrow (3a'')$$
$$\sigma\pi(A''); \quad (9a')(2a'') \rightarrow (3a'')^2$$
$$\sigma\sigma(A'); \quad (9a')(10a') \rightarrow (3a'')^2$$

Note that the $\pi\pi$ state is a four-π-electron (4π) system, while both the $\pi\sigma$ and $\sigma\pi$ have five π-electrons (5π). By the same token, the $\sigma\sigma$ state may be called a six-π-electron (6π) system.

Each diradical state can be either singlet or triplet. Besides, *trans* and *cis* configurations are possible for every state. Geometries of all these sixteen diradicals were optimized by the UHF SCF procedure. They were all confirmed to be planar in structure. The geometrical parameters are given in Tables 2 and 3 for the *trans* and *cis* configurations, respectively.

The total energies of the various diradical states were calculated by the MRD-CI procedure. The results expressed by taking the energy of the ground-state *trans*-HNOO as the standard are listed in Tables 2 and 3. Shown in Fig. 2 are the energy levels of these states. The levels for various combinations of the Σ and Δ states of the $NH + O_2$ system are also shown to illustrate the state

Table 2. Optimized geometries and the relative energies of the diradical states for *trans*-HNOO

	Singlet				Triplet			
	$^1\pi\pi$ (4π)	$^1\pi\sigma$ (5π)	$^1\sigma\pi$ (5π)	$^1\sigma\sigma$ (6π)	$^3\pi\pi$ (4π)	$^3\pi\sigma$ (5π)	$^3\sigma\pi$ (5π)	$^3\sigma\sigma$ (6π)
Geometry[a]								
R(N–O) (Å)	1.343	1.336	1.374	1.390	1.365	1.340	1.366	1.377
R(O–O) (Å)	1.290	1.378	1.274	1.372	1.315	1.367	1.268	1.380
R(H–N) (Å)	1.012	1.011	0.997	0.997	1.014	1.011	0.997	0.995
∠NOO (°)	111.4	106.7	111.9	105.6	108.1	106.6	113.4	104.1
∠HNO (°)	100.4	100.3	125.0	124.4	100.4	100.4	123.9	125.4
Relative energy[b]								
ΔE_{CI} (eV)	5.39	1.81	3.76	5.52	1.97	1.93	3.74	5.33

[a] 1 Å = 0.1 nm

[b] Relative to *trans*-HNOO($\tilde{X}^1A'$), for which $E_{CI} = -205.04677$ hartree

Table 3. Optimized geometries and the relative energies of the diradical states for *cis*-HNOO

	Singlet				Triplet			
	$^1\pi\pi$ (4π)	$^1\pi\sigma$ (5π)	$^1\sigma\pi$ (5π)	$^1\sigma\sigma$ (6π)	$^3\pi\pi$ (4π)	$^3\pi\sigma$ (5π)	$^3\sigma\pi$ (5π)	$^3\sigma\sigma$ (6π)
Geometry[a]								
R(N–O) (Å)	1.339	1.333	1.374	1.396	1.365	1.338	1.368	1.396[c]
R(O–O) (Å)	1.290	1.386	1.273	1.365	1.317	1.374	1.271	1.365[c]
R(H–N) (Å)	1.014	1.013	0.999	0.999	1.012	1.014	1.000	0.999[c]
∠NOO (°)	114.7	110.3	108.6	98.2	111.4	110.2	108.7	98.2[c]
∠HNO (°)	105.6	107.0	127.7	129.7	104.0	106.8	127.0	129.7[c]
Relative energy[b]								
ΔE_{CI} (eV)	5.03	1.94	4.14	4.78	1.76	2.02	3.97	5.56

[a] 1 Å = 0.1 nm

[b] Relative to *trans*-HNOO($\tilde{X}^1A'$), for which $E_{CI} = -205.04677$ hartree

[c] No stable UHF SCF minimum exists. The geometry parameters for $^1\sigma\sigma$ are assumed for CI calculations

correlations. The lowest excited state is apparently the triplet $\pi\pi$ state ($^3A'$) of the *cis* isomer. Further, for both the *trans* and *cis* isomers, the $\pi\sigma$ states are no doubt more stable by ca. 2 eV than the $\sigma\pi$ states. However, it does not seem possible to make any generalization as to the relative stabilities for the singlet vs. triplet excited states. Nor is it possible to conclude that the *trans* form of a given electronic state is generally more stable than the corresponding *cis* form.

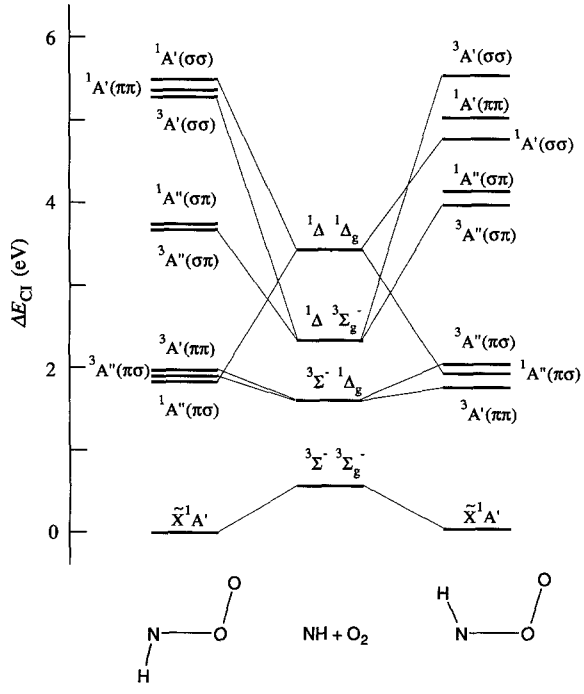

Fig. 2. Adiabatic excitation energies of the singlet and triplet HNOO diradicals. *trans*-HNOO($\tilde{X}^1A'$) is taken as the standard

3.3 Unimolecular reaction paths

Binkley et al. [13] considered theoretically the unimolecular decomposition pathway involving the ring closure of HNOO (**1**) followed by the O–O bond cleavage to give a symmetric (C_{2v}) HNO_2, hydrogen nitryl (**3**), which is a yet never identified entity. **3** would then suffer the isomerization into nitrous acid (**4**) as a direct precursor of NO and OH, which are to be formed in equal amounts.

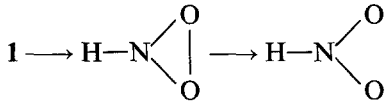

(3)

2 **3**

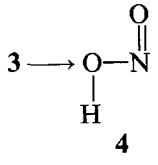

(4)

4

The reaction sequence **1** → **2** → **3** → **4** resembles the notable mechanism by which the methylene peroxide CH_2OO is believed to be led to formic acid HCOOH [14].

We here assume another pathway of decomposition that involves the 1,3-hydrogen migration giving rise to hydroperoxynitrene (**5**):

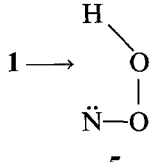

(5)

5

The singlet nitrene **5**, which has hitherto never been identified either, could also be a direct precursor of an equimolar mixture of NO and OH.

The minimum-energy path of Eq. (3) as well as Eq. (5) have been traced by the 6-electron/6-orbital MC SCF procedure. The optimal geometries of the transition states located, TS1 and TS2, respectively, for the initial ring closure in Eq. (3) and the 1,3-hydrogen migration (5) are illustrated in Fig. 3, together with those for the resulting ring isomer (**2**) and the singlet nitrene (**5**). It should be noted that TS1 was found to be connected with the *trans* form of the reactant HNOO, whereas TS2, with the *cis* structure by necessity.

The TS geometries were then dealt with by the MRD-CI procedure. The results are summarized in Table 4, together with the energy data obtained for the products **2** and **5**. The activation barrier heights were calculated to be 189 and 74 kJ/mol for TS1 and TS2, respectively. Clearly, the 1,3-hydrogen migration (5) is energetically more favorable than the ring closure in Eq. (3).

The subsequent isomerization/fragmentation processes were treated likewise. The overall potential energy profiles obtained are illustrated in Fig. 4. The ring-opening reaction of the cyclic intermediate (**2**) and the O–O bond cleavage of the nitrene (**5**) have both proved to have extremely low barriers (less than 10 kJ/mol). The transition state for the isomerization process **3** → **4**, i.e. Eq. (4), was found to be located ca. 96 kJ/mol *below* the ring entity (**2**). Thus, both the

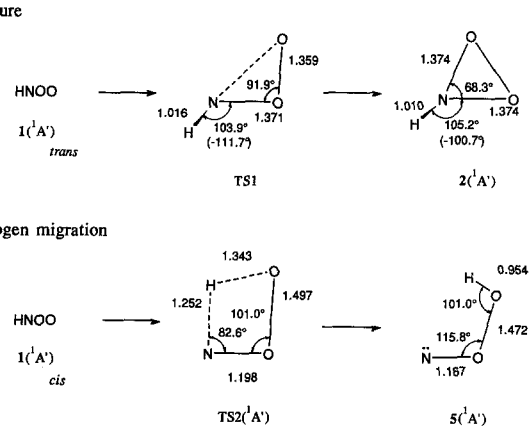

Fig. 3. Optimized (6-electron-6-orbital MC SCF/6-31G**) geometries for the transition states and products of the ring closure in Eq. (3) and the 1,3-hydrogen migration Eq. (5) of HNOO($\tilde{X}^1A'$). The bond lengths are given in units of Å. The data given in parentheses indicate the dihedral angles ϕ_{HNOO}

Table 4. Total energies calculated for the transition states and the products of unimolecular reactions of HNOO[a]

	Reaction (3)		Reaction (5)	
	TS1	**2**	TS2	**5**
Energies, $E + 204$ (hartree)				
RHF SCF	−0.40032	−0.49320	−0.45223	−0.52030
MC SCF	−0.52739	−0.56724	−0.54237	−0.61130
CI, $T \to 0$	−0.92600	−0.99390	−0.95992	−1.05399
CI, "full"	−0.97371	−1.03884	−1.01752	−1.10421
Relative energies, ΔE (kJ/mol)[b]				
CI	189	18	74	−154
CI + vib		16	62	−173

[a] Geometries are given in Fig. 3

[b] Relative to *cis*-HNOO($\tilde{X}^1A'$), for which $E_{CI} = -205.04563$ hartree

isomerization reactions related to TS1 and TS2 are the rate-determining step for the unimolecular decompositions of **1** giving NO + OH as ultimate products. Details of Eq. (4) will be reported elsewhere [15].

4 Discussion

As has already been mentioned, the binding energy of *cis*-HNOO (**1**) in the ground states is 48 kJ/mol. Therefore, the most favorable pathway of the HNOO decomposition, which involves the intermediacy of hydroperoxynitrene (**5**), is predicted to have a net activation barrier height of 26 kJ/mol against the initial binary system $NH(^3\Sigma^-) + O_2(^3\Sigma_g^-)$. When vibrational zero-point energy corrections are made, the binding energy is $E_0 = 27$ kJ/mol while the activation energy for Eq. (5) comes out to be $V_1 = 62$ kJ/mol. The net activation energy is then $E_0^{\ddagger} = V_1 - E_0 = 35$ kJ/mol. It has been verified in this connection that the initial association reaction has virtually no activation barrier. All these results merge into the statement that the overall reaction:

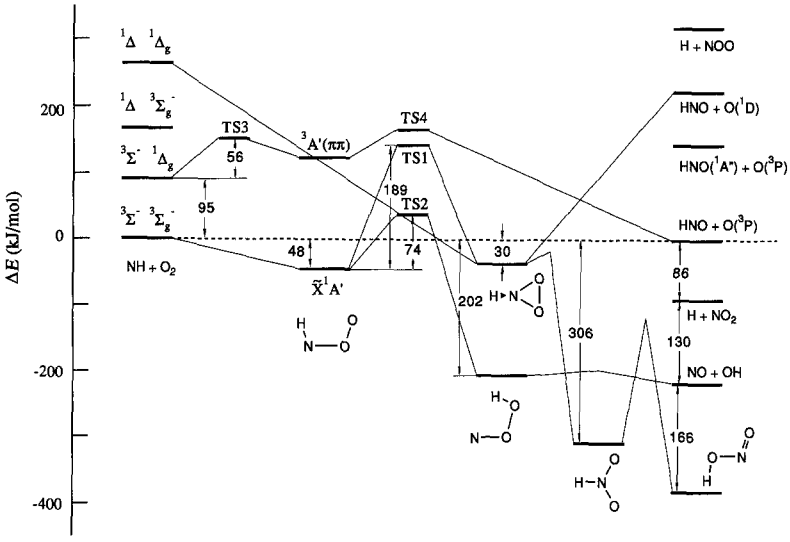

Fig. 4. Potential energy profiles calculated for the NH + O_2 system. The energy levels are based on the E_{CI} values. The energy gaps indicated are given in units of kJ/mol

$$NH(^3\Sigma^-) + O_2(^3\Sigma_g^-) \rightarrow NO + OH \tag{6}$$

should proceed through the rate-determining 1,3-hydrogen migration (5) with a net activation energy of 35 kJ/mol.

The activation energy calculated here for Eq. (6) is somewhat too large as compared to the experimental value of 6.4 kJ/mol determined by Hack et al. in the temperature range 286–543 K [4]. We believe that the discrepancy is an indication of the tunneling effect operative in the region of TS2. In what follows, we will consider this point quantitatively.

The overall reaction of our interest can be schematically represented as follows:

$$NH(^3\Sigma^-) + O_2(^3\Sigma_g^-) \underset{k_{-1}}{\overset{k_1}{\rightleftharpoons}} [HNOO]^* \xrightarrow{k_2} NO + OH \tag{7}$$

where [HNOO]* is the vibrationally hot adduct and where k_1 is a bimolecular rate constant while k_{-1} and k_2 are the unimolecular rate constants. Under the assumption that the second step (k_2) is rate-determining, the overall second-order rate constant k can be expressed as:

$$k = k_1(k_2/k_{-1})/[1 + (k_2/k_{-1})] \tag{8}$$

Since the initial association has no activation barrier, k_1 will be given by:

$$k_1 = (1/g_{NH}g_{O_2})Z \tag{9}$$

where g_{NH} and g_{O_2} are the electronic degeneracy factors of NH and O_2, respectively, both being 3 in the present instance, and where Z is the collision frequency. By assuming a classical collision diameter of 3.0 Å, k_1 is approximated to be $8.620 \times 10^{11} T^{1/2}$ cm^3 mol^{-1} s^{-1}. The rate constant ratio k_2/k_{-1} is considered to be governed not only by the difference in the relevant activation barrier heights but by the tunneling factor Γ involved in k_2. We here assume naively that:

$$k_2/k_{-1} = \Gamma\, e^{-\Delta E_0^{\ddagger}/RT} \tag{10}$$

as an upper bound.

In evaluating the tunneling correction factor Γ at the varying temperature, we have adopted Johnston's method [16] based on the Eckart potential model. Γ can be expressed as:

$$\Gamma = \frac{e^{V_1/RT}}{RT} \int_{E_0}^{\infty} \kappa(E)\, e^{-E/RT}\, dE \tag{11}$$

where $\kappa(E)$ is the one-dimensional penetration probability through the barrier at a given internal energy E. $\kappa(E)$ is a function of the Eckart potential parameters, V_1, V_2 and F^*. Here, V_1 and V_2 denote the heights of the barrier top above the reactant and product potential-energy minima, respectively, and F^* is the second derivative of the potential energy function at the barrier top. In the present instance, V_1 and V_2 are 62 and 235 kJ/mol, respectively, and $E_0 = 27$ kJ/mol. F^* is related to the imaginary frequency $\nu^{\ddagger}$ of the vibrational normal mode responsible to the motion of the hydrogen atom at TS2. The frequency obtained by the vibrational analysis of TS2 is $\nu^{\ddagger} = 2243i\ \mathrm{cm}^{-1}$.

The Γ values at various temperatures were calculated from Eq. (11) by numerical integration on a computer. The rate constants k calculated from Eqs. (8)–(10) by use of these Γ values are shown in Fig. 5. Effects of the tunneling are seen to be enormous at lower temperatures. The calculation results agree reasonably well with the experimental results reported by Hack et al. [4]. Further, the calculated curve fits both the experimental data obtained by Zetsch and Hansen at 296 K [2] and the value estimated by Dean et al. at 2000 K [17]. The apparent non-Arrhenius character of k can be rationalized most satisfactorily.

Finally, we will briefly comment on the reactions between NH and O_2 in the excited states. The lowest triplet state of HNOO(a^3A') will be formed by the addition of NH($^3\Sigma^-$) to $O_2(^1\Delta)$ with an activation barrier of 56 kJ/mol (TS3). With an additional energy of 9 kJ/mol (TS4), it will be collapsed into HNO + O:

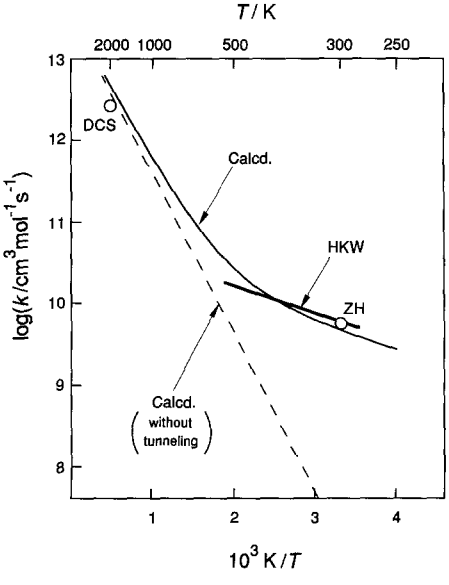

Fig. 5. Rate constants for the reaction $NH(^3\Sigma^-) + O_2(^3\Sigma_g^-) \rightarrow NO + OH$. *Full line*, calculated with the tunneling correction; *broken line*, calculated without the tunneling correction. Experimental data: ZH at 296 K [2]; HKW in the temperature range 286–543 K [4]. Estimated value: DCS at 2000 K [17]

$$NH(^3\Sigma^-) + O_2(^1\Delta) \rightarrow HNO + O(^3P) \quad (12)$$

Also, the reaction between $NH(^1\Delta)$ and $O_2(^1\Delta)$ will be a concerted cyloaddition to give the cyclic HNO_2 (**2**). It is to be readily isomerized into nitrous acid (**4**) via hydrogen nitryl (**3**), an intriguing planar symmetric isomer of **4**.

5 Conclusions

$HNOO(^1A')$ to be formed by the association between $NH(^3\Sigma^-)$ and $O_2(^3\Sigma_g^-)$ is a zwitter-ionic diradicaloid with a binding energy of only 27 kJ/mol (with the vibrational zero-point energy correction). The exchange reaction $NH(^3\Sigma^-) + O_2(^3\Sigma_g^-) \rightarrow NO + OH$ is predicted to proceed through the rate-determining isomerization of $HNOO(^1A')$ into hydroperoxynitrene, $NOOH(^1A')$. The net activation barrier height is calculated to be 35 kJ/mol (corrected for the zero-point energy). The bimolecular rate constants k calculated theoretically for the overall reaction by invoking the tunneling correction of the isomerization rate reproduce the non-Arrhenius variation of k observed over the temperature range 286–2000 K.

Acknowledgments. This work was supported by the Grant-in-Aid No. 62303002 from the Ministry of Education, Japan. The authors are grateful to Professor R. J. Buenker for supplying the Table MRD-CI program to them. All calculations were carried out on a HITAC M-680 at the Computer Center of the Institute for Molecular Science, Okazaki. The authors thank the Center for an allocation of CPU time.

References

1. a Fueno T, Bonačić-Koutecký V, Koutecký J (1983) J Am Chem Soc 105:5547–5557
   b Fueno T, Kajimoto O, Bonačić-Koutecký V (1984) J Am Chem Soc 106:4061–4062
   c Fueno T, Fukuda M, Yokoyama K (1988) Chem Phys 124:265–272
   d Fueno T (1988) J Mol Struct (Theochem) 170:143–149
   e Fueno T, Yamaguchi K, Kondo O (1990) Bull Chem Soc Jpn 63:901–912
2. Zetzsch C, Hansen I (1978) Ber Bunsen-Ges Phys Chem 82:830–833
3. Meaburn GM, Gordon S (1968) J Phys Chem 72:1592–1598
4. Hack W, Kurzke H, Wagner HGg (1985) J Chem Soc Faraday Trans 2 81:949–961
5. Yamaguchi K, Yabushita S, Fueno T (1979) J Chem Phys 71;2321–2322
6. GAUSSIAN 82, Binkley JS, Frisch MJ, DeFrees DJ, Raghavachari K, Whiteside RA, Schlegel HB, Pople JA (1984), Carnegie-Mellon University, Pittsburgh, PA; IMS version registered by Koga N
7. Hehre WJ, Ditchfield R, Pople JA (1972) J Chem Phys 56:2257–2261; Hariharan PC, Pople JA (1973) Theor Chim Acta 28:213–222
8. Buenker RJ (1982) In: Carbo R (ed) Studies in physicali and theoretical chemistry, vol 21. Elsevier, Amsterdam, p 17–34
9. Buenker RJ, Phillips RA (1985) J Mol Struct (Theochem) 123:291–300
10. Buenker RJ, Peyerimhoff SD (1974) Theor Chim Acta 35:33–58
11. Langhoff SR, Davidson ER (1974) Int J Quant Chem 8:61–72
12. Fueno T, Buenker RJ (19898) Theor Chim Acta 73:123–134
13. Melius CF, Binkley JB (1984) ACS Symp Ser 249; cited in Ref. [4]
14. Wadt WR, Goddard III WA (1975) J Am Chem Soc 97:3004–3021
15. Takane S, Fueno T, to be published
16. Johnston HS (1966) Gas phase reaction rate theory. Ronald Press, New York, p 40–47
17. Dean AM, Chou MS, Stern D (1984) Int J Chem Kinet 16:633–653